

# A UAV for Destructive Surveys of Mosquito Population

Mary Burbage, An Nguyen, Kyle Walker, Nhan Phung, Vinh Truong, Erik Van Aller, and Aaron T. Becker

**Abstract**—This paper introduces techniques for mosquito population surveys in the wild using electrified screens (bug zappers) mounted to a UAV. Instrumentation on the UAV logs the UAV path and the GPS location, altitude, and time of each mosquito elimination. Changing the path of the UAV changes the number of mosquitos encountered. We pose this as a new problem in robotic coverage and provide a simulator for mosquitos swarms and a UAV with a screen. We compare four baseline algorithms. Hardware experiments with a UAV equipped with an electrified screen provide real-time measurements of (former) mosquito locations and mosquito-free volumes.

## I. INTRODUCTION

Mosquito-borne diseases kill millions of humans each year [1]. Because of this threat governments worldwide track mosquito populations. Tracking individual mosquitos is difficult because of their small size, wide-ranging flight, and preference for low-light. Tracking studies have chosen to use small (1.2 x 2.4 m) indoor regions [2], or of mating swarms outdoors [3].

The dominant tools for tracking mosquito populations are stationary traps that are checked at weekly intervals (Encephalitis Vector Surveillance traps and/or gravid traps [4]). Recent research has focused on making these traps smaller, cheaper, and provide real-time data [5].

microsoft research paper on drone delivery of traps (U Penn)?

However, they still rely on attracting mosquitos to the trap. This paper presents an alternate solution using electrified bug zappers mounted on a UAV. As the UAV follows a path it sweeps out a volume of air, temporarily removing all the mosquitos in this volume. By monitoring the voltage across this screen we can track individual mosquito contacts.

new image of drone and screen. must have scale bars and annotation. Must have downward facing camera

The paper is arranged as follows. After a review of related work, We present a design and rationale for a UAV with bug zapper. We introduce a new robotic coverage problem in We present a benchmark simulation for comparing trajectories Followed by simulation results comparing four baseline

M. Burbage, A. Nguyen, K. Walker, N. Phung, V. Truong, E. Van Aller, and A. Becker are with the ECE Department at the University of Houston, TX. [atbecker@uh.edu](mailto:atbecker@uh.edu).



Fig. 1. A hexcopter drone carrying a 60 cm square bug-zapping screen. An onboard microcontroller monitors the voltage across the screen and records the time, GPS location, and altitude for each mosquito strike. Video is available at <https://youtu.be/1gvJ-yTf-E8> [6].

simulations. We then present hardware experiments with the UAV and conclude with directions for future research.

Here we discuss simulations of a large number of mosquitoes within a rectangular area. Each mosquito obeys a biased random walk flight pattern. The flying robot follows a set of four path plans and can eliminate any modeled mosquito that intersects its path, detect the time each mosquito is eliminated, and use this data as feedback for a motion policy. After setting a benchmark with modeled mosquitoes and robots, we describe a prototype multi-copter and screen.

## II. RELATED WORK

### A. Robotic coverage

Robotic coverage has a long history. The basic problem is one of designing a path for a robot that ensures the robot visits within  $r$  distance of every point on the workspace. For an overview see [7]. This work has been extended to use multiple coverage robots in a variety of ways, including using simple behaviors for the robots [8], [9]. The key difference in the mosquito coverage problem is that the mosquitoes can move, recontaminating an area previously cleared. We instead have a probability of coverage, as in [10]. This is closely related to the art gallery problem [11] but with limited range of visibility.

This process can be modeled as sampling without replacement from a point cloud of mobile particles using a

mobile agent. The point cloud particles are generated from a known or unknown distribution, and the mobile agent clears all particles in a swept-out region each time step. UAVs have strict energy budgets, which limit the flight time. The goal is to design a trajectory with duration  $\leq T$  that, in probability, samples the most particles. We assume the agent can detect each particle collision, which the agent can use to modify a planned trajectory. This paper presents both open-loop trajectories and policies with feedback.

### B. Mosquito Control Solutions

Mosquito control has a long history of efforts associated both with monitoring mosquito populations [12] and with eliminating mosquitoes. The work involves both draining potential breeding grounds and destroying living mosquitoes [13]. An array of insecticidal compounds has been used with different application methods, concentrations, and quantities, including both larvicides and compounds directed at adult mosquitoes [14].

Traditional electrified screens (bug zappers) use UV light to attract pests but have a large bycatch of non-pest insects [15].

Various traps have been designed to capture and/or kill mosquitoes with increasing sophistication in imitating human bait as designers strive to achieve a trap that can rival the attraction of a live human [16]. In recent history, methods have also included genetically modifying mosquitoes so that they either cannot reproduce effectively or cannot transmit diseases successfully [17], and with the recent genomic mapping of mosquito species, new ideas for more targeted work have been formulated [18].

Popular methods to control mosquitoes such as insecticides are effective, but they have the potential to introduce long-term environmental damage and mosquitoes have demonstrated the ability to become resistant to pesticides [19]. Traditional electrified screens (bug zappers) use UV light to attract pests but have a large bycatch of non-pest insects [15]. This paper introduces techniques using bug zappers mounted on unmanned vehicles to autonomously seek out and eliminate mosquitoes in their breeding grounds and swarms. Instrumentation on the bug zappers logs the GPS location, altitude, weather details, and time of each mosquito hit. Mosquito control offices can use this information to analyze the insects' activities. The device can be mounted on a remote-controlled or autonomous unmanned vehicle. If autonomous, the vehicle can use the data collected from the electrified screen as feedback to improve the effectiveness of the motion plan.

### C. Robotic Pest Management

As GPS technology has flourished and data processing has become cheaper and more readily available, researchers have explored options for implementing the new technologies in breeding ground removal [20] and more effective insecticide dispersion [21]. Low cost drones for residential spraying are under development [22]. Even optical solutions have been considered, including laser containment [23] or, by

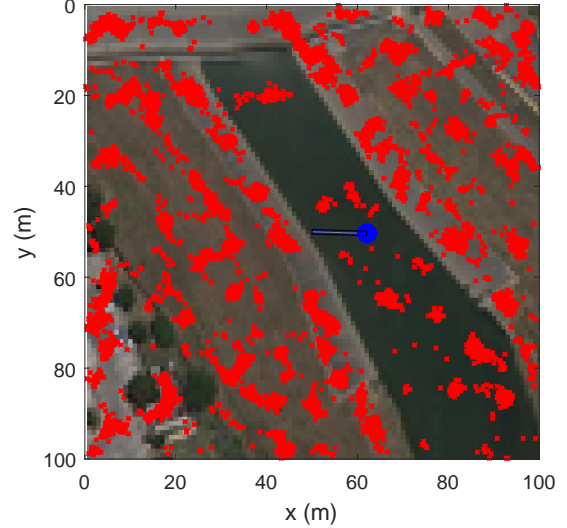


Fig. 2. A  $100\text{ m} \times 100\text{ m}$  image with one thousand simulated mosquitoes (red markers). The mosquitoes have had 1.4 hours to bias themselves toward green areas of the image. The robot (blue circle) is shown in the center, preparing to start a bug-zapping run.

extension, exclusion and laser tracking and extermination [24].

## III. SIMULATION

Before launching a fully-instrumented drone, this concept was simulated using MATLAB code, which is available at [25]. Ten thousand mosquitoes are randomly placed within a square area one hundred meters on a side. A satellite image of Houston was used as the simulation environment, and each mosquito is programmed to move according to a biased random walk at a speed up to  $0.4\text{ m/s}$  and with a direction heading biased toward the greenest of the pixels surrounding its current position. This imitates the live mosquitoes' preference for vegetative areas.

The simulation is initialized by a mosquito distribution generated by running the mosquito movement routine five thousand times, simulating 1.4 hours of flying time, before the robot begins to search. Because mosquitoes do not care about boundaries, a toroidal mapping is used to keep them in the workspace. Fig. 11 shows the biased mosquitoes.

The robot is tested with four different paths. The first is a plain boustrophedon or lawn-mowing path [7]. The robot begins in one corner of the workspace and methodically progresses back and forth, advancing one screen width at each turn. If it covers the entire field in the allotted time, it begins covering the field again.

The second uses a random bounce algorithm. The robot begins in the center of the workspace and moves with a heading that varies randomly up to  $\pm 0.2\text{ rad}$  from its previous heading and bounces off the perimeter of the workspace with a random heading equally biased between  $0$  and  $2\pi\text{rad}$ , excluding headings leading outside the workspace.

The third path begins with the boustrophedon path but switches to a square spiral path when the rate of mosquito kills exceeds a threshold. Once the kill rate falls below another threshold, the path returns to a boustrophedon path. The final path combines the random bounce path with the square spiral in the same way as the third path.

For the main body of the simulation, a loop runs a series of iterations in which each mosquito moves one step and the robot moves one step. In that step, the path traced by the bug-zapping screen is calculated, and any mosquitoes in that path are considered to have been counted and killed.

To keep the routines comparable, the robots use the same speed and same number of iterations in each test as well as the same image for biasing the mosquito flight. The baseline simulations used  $12 \text{ m/s}$  and fifteen minutes of flying time, which is enough time for the robot to completely cover the  $100\text{m}$  workspace.

One hundred trials were performed with each coverage path and the results evaluated. The boustrophedon successfully covered the entire field in every trial ( $\mu = 100\%$ ,  $\sigma = 0\%$ ), while the random bounce covered only 64.7% of the field ( $\mu = 64.7\%$ ,  $\sigma = 1.1\%$ ) on average. The boustrophedon with spiral covered 91.5% of the field ( $\mu = 91.5\%$ ,  $\sigma = 0.6\%$ ), and the random bounce with spiral covered 66.0% ( $\mu = 66.0\%$ ,  $\sigma = 1.3\%$ ). Due to the higher coverage rates, the boustrophedon killed significantly more mosquitoes ( $\mu = 84.9\%$ ,  $\sigma = 0.4\%$ ) than the random bounce ( $\mu = 65.9\%$ ,  $\sigma = 2.5\%$ ), though the addition of the spiral to the random bounce showed an improvement over the plain random bounce ( $\mu = 71.9\%$ ,  $\sigma = 3.8\%$ ). Including the spiral with the boustrophedon degraded its performance ( $\mu = 79.8\%$ ,  $\sigma = 1.7\%$ ). Fig. 3 and Fig. 4 show the paths for the baseline trials and their success rates, respectively.

Having set a baseline in which full coverage was clearly the best method, we next considered the problem of a field which is too large for full coverage within the allotted time. To simulate this, we used the same environment but set the flight time to five minutes and repeated the hundred iterations of each method.

With reduced flying time, the coverage and kill rates were much lower than in the baseline tests, but the spiral improved the kill rate for both the boustrophedon and the random bounce paths. Sample paths are displayed in 5. Results are illustrated in Fig.6, which shows the best kill rate of 35.0% ( $\mu = 35.0\%$ ,  $\sigma = 3.0\%$ ) for the boustrophedon with spiral path, followed by the random bounce with spiral path at 32.5% ( $\mu = 32.5\%$ ,  $\sigma = 3.5\%$ ). The boustrophedon and random bounce paths had equal kill rates of 31.2%, though the boustrophedon had a narrower standard distribution ( $\mu = 31.2\%$ , boustrophedon:  $\sigma = 0.5\%$ , random bounce:  $\sigma = 2.8\%$ ). It also covered a greater percentage of the workspace than the random bounce, 35.7% as opposed to 30.6%. We consider this a benchmark against which testing of new methods may be measured in the future.

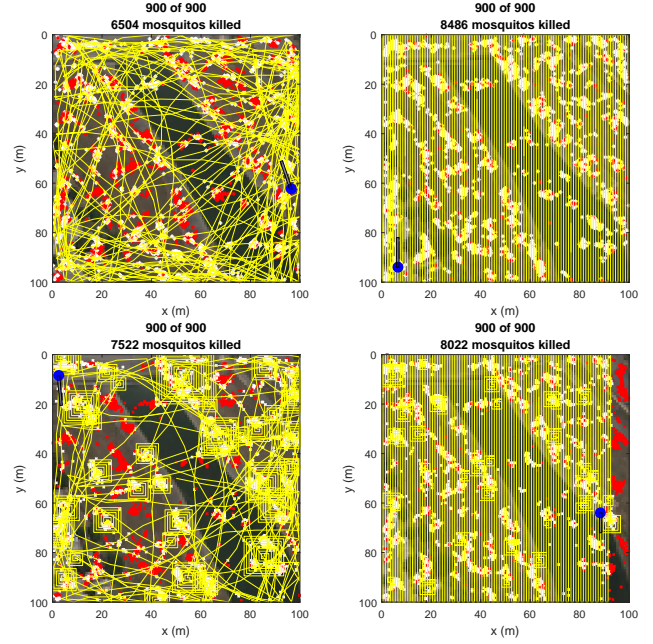


Fig. 3. Four sample simulations. The robot (blue circle) and the area covered by the bug-zapping net in an iteration (blue rectangle) are shown along with a population of ten thousand mosquitoes. Those killed during the simulation are white, and those that survived are red. Left column random bounce, right column boustrophedon. Bottom row adds a subroutine to perform spiral movements when the mosquito density is high.

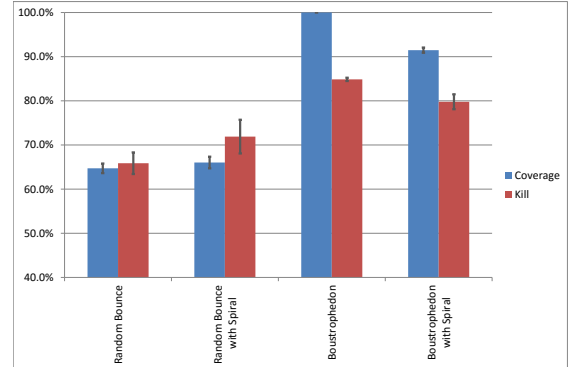


Fig. 4. Comparison of percentage of area covered and percentage of mosquitoes killed in fifteen minutes for the four coverage patterns. Plots show aggregate results of 100 trials, using the workspace shown in Fig. 11.

#### IV. HARDWARE DESIGN

This section examines the components of the mosquito drone system, shown in Fig. 1. This includes the electronics, electrified screen, energy budget, UAV, and design parameters. The design for the mosquito drone system has been assigned U.S. Provisional Patent Application [26].

##### A. Electronics

The system is powered by a 9 V Lithium Ion battery applied directly to the controller and two AA 3 V Lithium Ion batteries applied to the power circuit for the screen. The

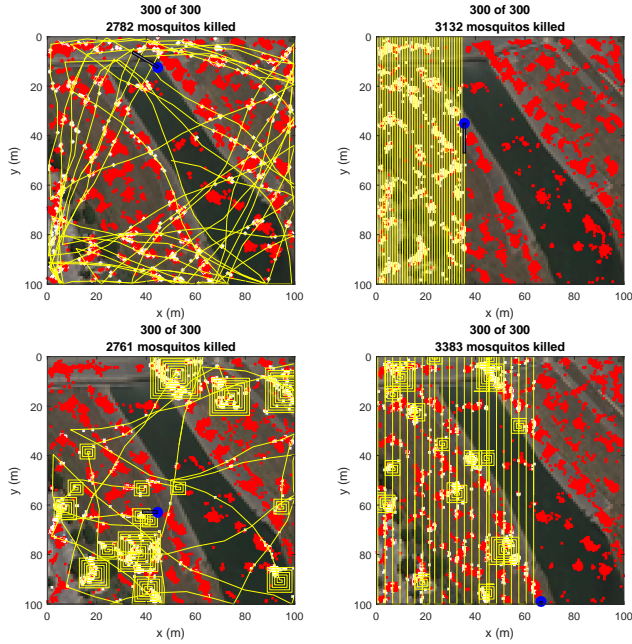


Fig. 5. Left column random bounce, right column boustrophedon. Bottom row adds a subroutine to perform spiral movements when the mosquito density is high.

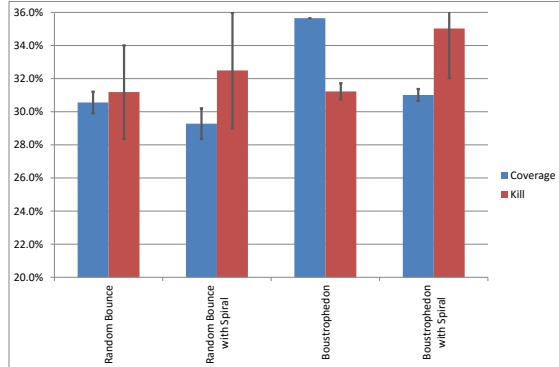


Fig. 6. Comparison of percentage of area covered and percentage of mosquitoes killed in five minutes for the four coverage patterns. Plots show aggregate results of 100 trials, using the workspace shown in Fig. 11.

power circuit outputs a high DC voltage across the screen. A protection circuit, shown in Fig. 7, steps this voltage down to a suitable level for monitoring by the ADC of the controller. The controller uses a GPS shield for monitoring the location and altitude as well as a real time clock to timestamp each data point collected from the system.

The power circuit uses a BJT and center tap transformer to invert a DC input voltage to AC and apply it to the primary winding of a step-up transformer. The voltage at the secondary winding of the transformer is boosted and rectified to two high voltage output capacitors. The protection circuit utilizes a voltage divider to reduce the voltage to a level suitable for the controller, this divider utilizes a

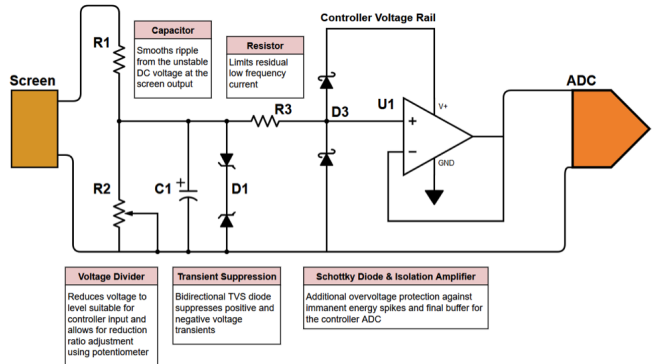


Fig. 7. Circuit diagram of the bug zapper and probe circuit.

potentiometer to adjust the ratio of screen output voltage and the voltage seen by the controller. A capacitor is used at the input of this circuit to smooth the unstable DC voltage at the screen output. A small series resistor is also used to limit residual low frequency current. A bidirectional transient voltage suppression (TVS) diode is then used to restrict both positive and negative high voltage transients that will propagate through the divider and capacitor. Buffering the controller are a Schottky diode and isolation amplifier. Both are powered by the controller supply rail and are used to protect against imminent voltage spikes that would destroy the TVS diode.

### B. Screen

new description of screen

The screen is constructed with two layers of wire mesh with 3.6 mm openings with a layer of wire mesh with 0.74 mm openings suspended between them. A balsa wood frame insulates the outer meshes from the inner mesh. This mesh arrangement weighs 1633 g/m<sup>2</sup>. The payload that the drone can reliably carry is used to select a size that satisfies the requirements, 60 cm for this multi-copter drone.

### C. Drone

describe the drone

### D. Energy Budget

what is the new energy usage of the screen?

Tests with an oscilloscope show that in the steady state, a 60 cm × 60 cm screen and electronics have a power consumption of 3.6 W. During a zap, the screen voltage monitoring circuit shorts briefly when the mosquito contacts the screen. Fig. 8 shows the time sequences for battery and screen voltages, current, and power during five mosquito

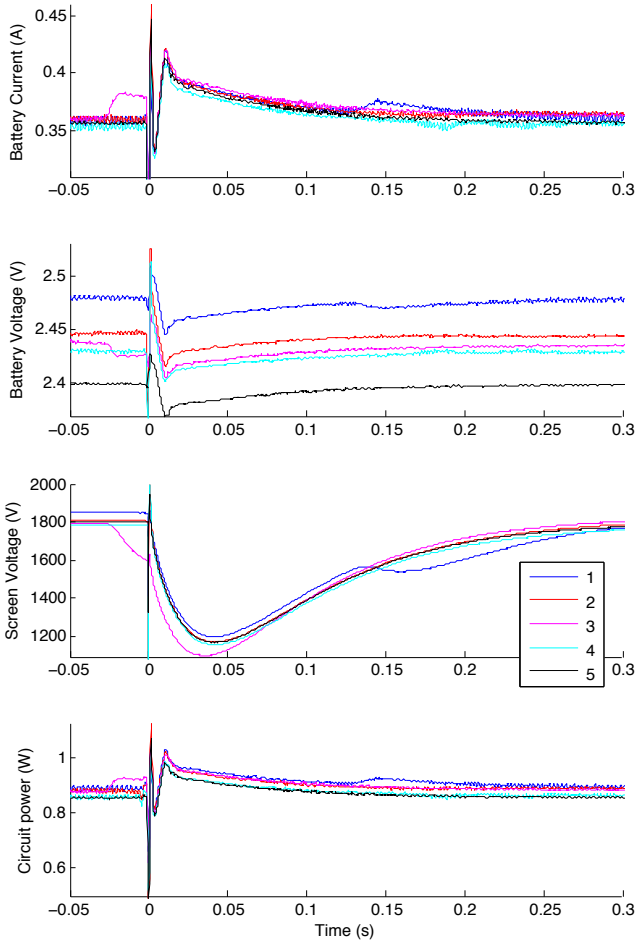


Fig. 8. Current, voltage, and power traces for five *Culex quinquefasciatus* mosquitoes as each contacts the bug-zapping screen. Contact causes a brief short that recovers in 160 ms.

zaps. The initial current spike recovery can be modeled with an exponential fit.

$$i = 69.1e^{-2.7 \times 10^4 t} A \quad (1)$$

The fit in (1) gives us a time constant of  $2.7 \times 10^4 / s$  for the short and a recovery time of 80  $\mu s$ . Multiplying voltage by current to find the instantaneous power ( $p = iv$ ) and integrating the area under the power curve show a total energy consumption of 4.2 mJ for each zap. Recharging the screen requires more power and is represented in the latter part of the curves. The overall recovery time is about 160 ms. Most of the energy is consumed charging and maintaining the charge on the screen rather than in zapping the mosquitoes.

#### E. Location of screen

The drone carries the bug-zapping screen, which is suspended by fishing line at each corner. The location of this screen determines the efficacy of the mosquito drone, measured in mosquitoes eliminated per second of flight time.

For manufacturing ease, the electrified screen is a square measuring  $d_s$  on each side. The mosquito species we are ini-

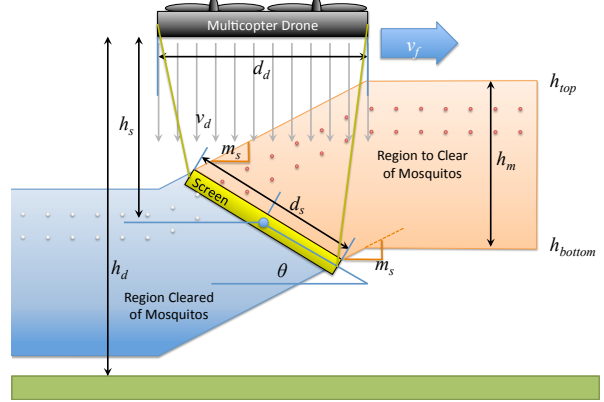


Fig. 9. The drone suspends a rectangular bug-zapping screen beneath it. Propwash pushes incoming mosquitoes downwards, and the drone clears a volume  $h_m \times d_s \times v_f$ . Circles show two mosquitoes at equal time intervals relative to the drone.

tially targeting fly at low altitude, so the screen is suspended a distance  $h_s$  beneath the drone flying at height  $h_d$ . Suspending this screen beneath the drone improves efficiency because a hanging screen requires less weight than a rigid frame to hold the screen above the drone. This screen can be suspended at any desired angle  $\theta$  in comparison to horizontal, as shown in Fig. 9. A key question is what distance  $h_s$  the screen should be suspended from the drone, and the optimal angle  $\theta$ . The goal is to clear the greatest volume of mosquitoes per second, a volume defined by the drone forward velocity  $v_f$  and the cross sectional area  $h_m \times d_s$  cleared by the screen, as shown in Fig. 10.

To hover, the drone must push sufficient air down with velocity  $v_d$  to apply a force that cancels the pull of gravity. The drone has mass  $m_d$  and its cross section can be approximated as square-shaped with size  $d_d \times d_d$ . The mass flow of air through the drone's props is equal to the product of the change in velocity of the air, the density of the air  $\rho_a$ , and the cross sectional area.

We assume that air above the drone is quiescent, so the change in velocity of the air is  $v_d$  m/s.

$$\begin{aligned} \text{Force gravity} &= (\text{mass flow}) \cdot \text{air velocity} \\ m_d \cdot g &= (v_d \cdot \rho_a \cdot d_d^2) \cdot v_d \end{aligned} \quad (2)$$

Then the required propwash, the velocity of air beneath the drone, for hovering is

$$v_d = \sqrt{\frac{m_d g}{\rho_a d_d^2}} \quad (3)$$

The flight testing site in Houston, Texas is 15m above sea level. At sea level the density of air  $\rho_a$  is 1.225 kg/m<sup>3</sup>. The drone weighs 5.1 kg with a width of 0.74 m [27]. The acceleration due to gravity is 9.871 m/s<sup>2</sup>. Substituting these values into (3) gives  $v_d = 8.5$  m/s.

Due to propwash, an initially hovering mosquito will fall when under the drone at a rate of  $v_d$ . Relative to the drone the mosquito moves horizontally  $-v_f$ . As shown in Fig. 9, we

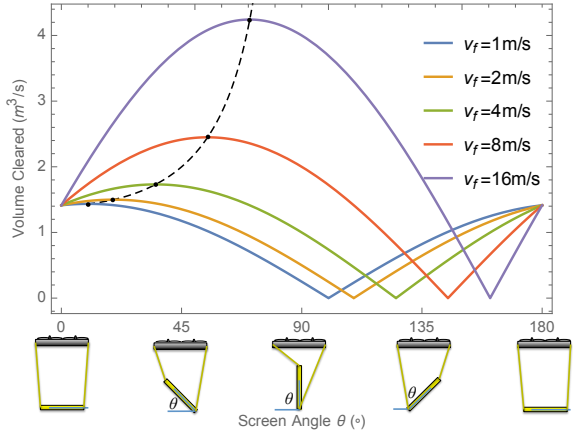


Fig. 10. The volume cleared by a drone is a function of screen angle  $\theta$  and forward velocity  $v_f$ . The dotted line shows the optimal angle given in (5).

can extend lines with slope  $v_d/v_f$  from the screen's trailing edge to  $h_{top}$  and from the leading edge to  $h_{bottom}$

$$\begin{aligned} h_{top} &= h_d - h_s + \frac{d_s}{2} \sin(\theta) + \frac{d_d + d_s \cos(\theta)}{2} \frac{v_d}{v_f} \\ h_{bottom} &= h_d - h_s - \frac{d_s}{2} \sin(\theta) + \frac{d_d - d_s \cos(\theta)}{2} \frac{v_d}{v_f} \\ h_m &= h_{top} - h_{bottom} = d_s \left( \frac{v_d}{v_f} \cos(\theta) + \sin(\theta) \right) \end{aligned} \quad (4)$$

The optimal angle is therefore a function of forward and propwash velocity:

$$\theta = \text{ArcTan} \left( \frac{v_f}{v_d} \right) \quad (5)$$

To ensure the maximum number of mosquitoes are collected, the screen must be sufficiently far below the drone  $h_s > \frac{d_s}{2} \sin(\theta) + \frac{d_d + d_s \cos(\theta)}{2} \frac{v_d}{v_f}$  and the bottom of the screen must not touch the ground,  $h_d > h_s + \frac{d_s}{2} \sin(\theta)$ .

Tests with  $h_s > 2$  m were abandoned because the long length caused the screen to act as a pendulum, introducing dynamics that made the system difficult to fly.

Changing the flying height  $h_d$  of the drone will target different mosquito populations because mosquitoes are not distributed uniformly vertically. Gillies and Wilkes have demonstrated that different species of mosquitoes prefer to fly at different heights [28].

## V. SIMULATION

See benchmarking code at [25]. Before launching a fully-instrumented drone, this concept was simulated using MATLAB code. One thousand mosquitoes are randomly placed within a square area one hundred meters on a side. A satellite image of Houston was used as the simulation environment, and each mosquito is programmed to move according to a biased random walk at a speed up to 0.4 m/s and with a direction heading biased toward the greenest of the pixels surrounding its current position. This imitates the live mosquitoes' preference for vegetative areas. The

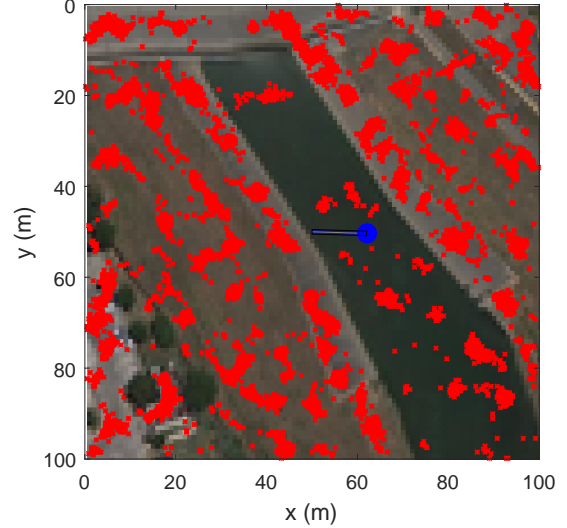


Fig. 11. A 100 m × 100 m image with one thousand simulated mosquitoes (red markers). The mosquitoes have had 1.4 hours to bias themselves toward green areas of the image. The robot (red circle) is shown at the upper left corner, preparing to start a bug-zapping run.

simulation is initialized by a mosquito distribution generated by running the mosquito movement routine five thousand times, simulating 1.4 hours of flying time, before the robot begins to search (Fig. 11). Because mosquitoes do not care about boundaries, a toroidal mapping is used to keep them in the workspace.

Two different routines handle the robot's path. The first uses a random bounce algorithm. The robot begins in the center of the workspace and moves with a heading that varies randomly up to  $\pm 0.2$  rad from its previous heading and bounces off the perimeter of the workspace with a random heading equally biased between 0 and  $2\pi$ , excluding headings leading outside the workspace. The velocity is set at a prescribed speed.

The second algorithm uses a boustrophedon path [7]. The robot begins in one corner of the workspace and methodically progresses back and forth, advancing one screen width at each turn. If it covers the entire field in the allotted time, it begins covering the field again.

To keep the routines comparable, the robots use the same speed and same number of iterations. These simulations used 12 m/s and fifteen minutes of flying time. They also used the same image for biasing the mosquito flight.

For the main body of the simulation, a loop runs a series of iterations in which each mosquito moves one step and the robot moves one step. In that step, the path traced by the bug-zapping screen is calculated, and any mosquitoes in that path are considered to have been killed.

One hundred trials were performed with each coverage path and the results evaluated. The boustrophedon successfully covered the entire field in every trial ( $\mu = 100\%$ ,  $\sigma = 0\%$ ) and covered a portion of the area a second time, while the random bounce covered only 67.9% of the field

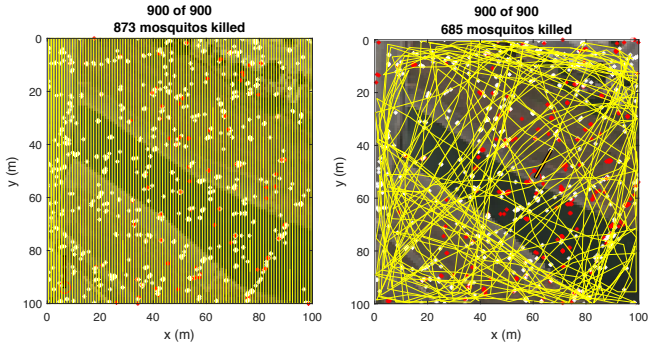


Fig. 12. Boustrophedon robot (left) and random bounce (right) path (yellow lines) overlaid upon a  $100\text{ m} \times 100\text{ m}$  image. The robot (red circle) and the area covered by the bug-zapping screen in an iteration (red rectangle) are shown along with a population of a thousand mosquitoes. Those killed during the simulation are white, and those that survived are red.

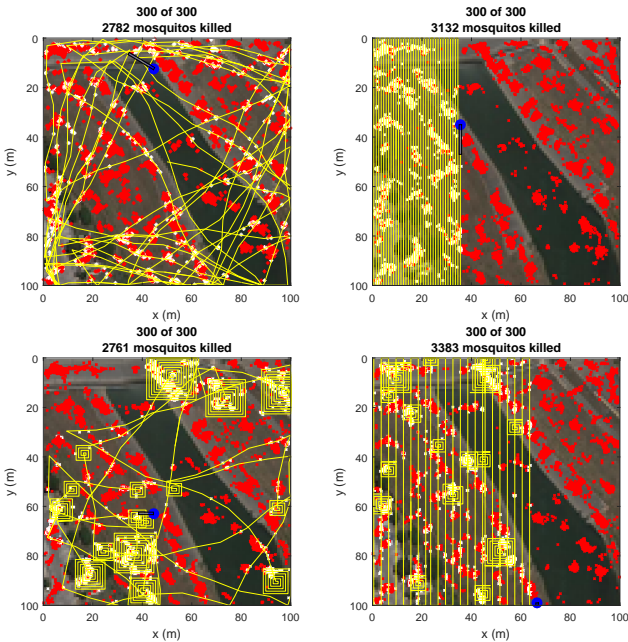


Fig. 13. Left column random bounce, right column boustrophedon. Bottom row adds a subroutine to perform spiral movements when the mosquito density is high.

$(\mu = 67.9\%, \sigma = 1.0\%)$  with a considerable amount of overlap. As a result, the boustrophedon killed significantly more mosquitoes ( $\mu = 87.7\%, \sigma = 1.1\%$ ) than the random bounce ( $\mu = 68.6\%, \sigma = 2.7\%$ ). In fact, the smallest number of mosquitoes killed in 100 trials by the boustrophedon (84.1%) was considerably larger than the largest number killed by the random bounce (75.1%). Fig. 13 show sample paths for boustrophedon and random bounce trials.

## VI. EXPERIMENTS

replace with the new experiment description

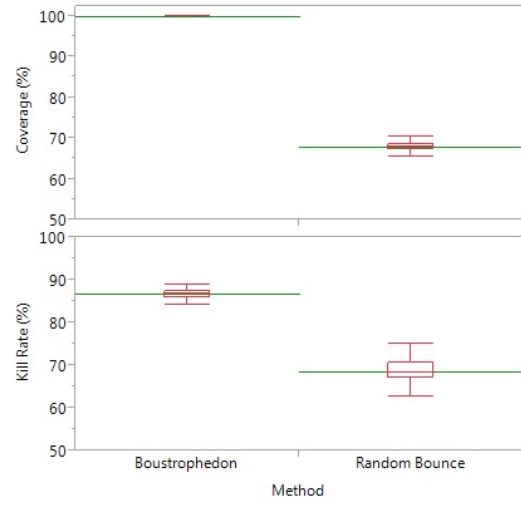


Fig. 14. Comparison of percentage of area covered and percentage of mosquitoes killed for the boustrophedon and random bounce coverage patterns. Plots show aggregate results of 100 trials, using the workspace shown in Fig. 11.

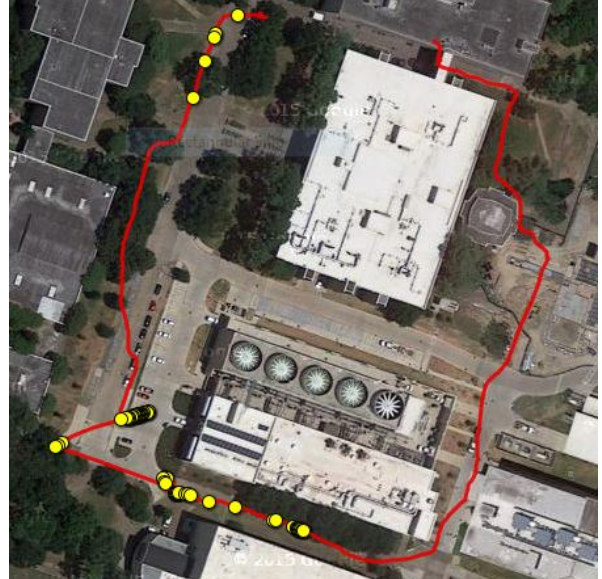


Fig. 15. Satellite image overlaid with GPS path (red line) and kill locations (yellow circles) from proof of concept trial. Visualization using [29].

Simulation has shown that covering the field thoroughly leads to a higher success rate when killing mosquitoes. Because the mosquitoes move around, the robot will not kill all the mosquitoes in a single trial as some can fly into a previously covered area as the robot approaches them; however, the chances of killing the mosquitoes increase as the coverage increases.

## VII. CONCLUSION AND FUTURE WORK

This paper presented a new problem in robotic coverage that attempts to maximize the number of moving particles detected when they are sampled without replacement. We provided a benchmark simulation and showed that techniques exist that outperform a simple boustrophedon search.

Initial experiments with the UAV and electrified screen track the location of a mosquito-killing drone as it patrols a field and map mosquito kills.

There are a number of refinements to the simulation algorithm that could be pursued in future work. Refinements are possible in both the mosquito-biasing algorithm and the robot flight simulation. The model may be expanded to three dimensions. Additional search paths may be compared to the existing algorithms. These and other considerations will make a more realistic model for future work. Full instrumentation of the multi-copter drone will allow more extensive testing of the hardware design and will allow field tests of the simulation algorithms.

New sensors are being developed that can identify and detect flying insects, [5]. These sensors may enable a drone to proactively steer toward insect swarms and identify insects in realtime.

For a non-destructive population survey, the screen could be replaced with a net and, with appropriate lighting, the camera used to record capture events.

Teams of UAVs could work together to map areas more quickly and measure gradients of the distribution to quickly find large mosquito populations.

#### ACKNOWLEDGMENT

The authors acknowledge the helpful advice and feedback from Martin Reyna Nava, MS, Medical Entomologist and Technical Operations Manager and Mustapha Debboun, Ph.D, BCE, Director Mosquito Control Division, of the Harris County Public Health & Environmental Services, Mosquito Control Division.

This material is based upon work supported by the National Science Foundation under Grant No. IIS-1553063. Any opinions, findings, and conclusions or recommendations expressed in this material are those of the authors and do not necessarily reflect the views of the National Science Foundation.

#### REFERENCES

- [1] C. J. Murray, L. C. Rosenfeld, S. S. Lim, K. G. Andrews, K. J. Foreman, D. Haring, N. Fullman, M. Naghavi, R. Lozano, and A. D. Lopez, "Global malaria mortality between 1980 and 2010: a systematic analysis," *The Lancet*, vol. 379, no. 9814, pp. 413–431, 2012.
- [2] J. E. Parker, N. Angarita-Jaimes, M. Abe, C. E. Towers, D. Towers, and P. J. McCall, "Infrared video tracking of anopheles gambiae at insecticide-treated bed nets reveals rapid decisive impact after brief localised net contact," *Scientific reports*, vol. 5, 2015.
- [3] S. Butail, N. Manoukis, M. Diallo, A. S. Yaro, A. Dao, S. F. Traoré, J. M. Ribeiro, T. Lehmann, and D. A. Paley, "3d tracking of mating events in wild swarms of the malaria mosquito anopheles gambiae," in *2011 Annual International Conference of the IEEE Engineering in Medicine and Biology Society*. IEEE, 2011, pp. 720–723.
- [4] G. M. Williams and J. B. Gingrich, "Comparison of light traps, gravid traps, and resting boxes for west nile virus surveillance," *Journal of Vector Ecology*, vol. 32, no. 2, pp. 285–291, 2007.
- [5] Y. Chen, A. Why, G. Batista, A. Mafra-Neto, and E. Keogh, "Flying insect classification with inexpensive sensors," *Journal of insect behavior*, vol. 27, no. 5, pp. 657–677, 2014.
- [6] A. Nguyen. (2016, Mar.) Uav with instrumented bug zapper. [Online]. Available: <https://youtu.be/lgv1-yTf-E8>
- [7] H. Choset, "Coverage for robotics - a survey of recent results," *Annals of Mathematics and Artificial Intelligence*, vol. 31, no. 1-4, pp. 113–126, October 2001.
- [8] D. Spears, W. Kerr, and W. Spears, "Physics-based robot swarms for coverage problems," *The international journal of intelligent control and systems*, vol. 11, no. 3, 2006.
- [9] S. Koenig, B. Szymanski, and Y. Liu, "Efficient and inefficient ant coverage methods," *Annals of Mathematics and Artificial Intelligence*, vol. 31, no. 1, pp. 41–76, Oct. 2001.
- [10] C. Das, A. Becker, and T. Bretl, "Probably approximately correct coverage for robots with uncertainty," in *IEEE/RSJ International Conference on Intelligent Robots and Systems (IROS)*, vol. 1, San Francisco, CA, USA, Oct. 2011, pp. 1160–1166.
- [11] D.-T. Lee and A. K. Lin, "Computational complexity of art gallery problems," *Information Theory, IEEE Transactions on*, vol. 32, no. 2, pp. 276–282, 1986.
- [12] J. A. Dennett, A. Bala, T. Wuithiranyagool, Y. Randle, C. B. Sargent, H. Guzman, M. SIIRIN, H. K. Hassan, M. Reyna-Nava, T. R. Unnasch *et al.*, "Associations between two mosquito populations and west nile virus in harris county, texas, 2003–06," *Journal of the American Mosquito Control Association*, vol. 23, no. 3, p. 264, 2007.
- [13] R. Peter, P. Van den Bossche, B. L. Penzhorn, and B. Sharp, "Tick, fly, and mosquito control—lessons from the past, solutions for the future," *Veterinary parasitology*, vol. 132, no. 3, pp. 205–215, 2005.
- [14] W. H. Organization, "Guidelines for laboratory and field testing of mosquito larvicides," *WORLD HEALTH ORGANIZATION COMMUNICABLE DISEASE CONTROL, PREVENTION AND ERADICATION WHO PESTICIDE EVALUATION SCHEME*, 2005.
- [15] sciencedaily.com. (1997, Jul.) Snap! crackle! pop! electric bug zappers are useless for controlling mosquitoes, says uf/ifas pest expert. [Online]. Available: <http://www.sciencedaily.com/releases/1997/07/970730060806.htm>
- [16] D. V. Maliti, N. J. Govella, G. F. Killeen, N. Mirzai, P. C. Johnson, K. Kreppel, and H. M. Ferguson, "Development and evaluation of mosquito-electrocuting traps as alternatives to the human landing catch technique for sampling host-seeking malaria vectors," *Malaria journal*, vol. 14, no. 1, p. 1, 2015.
- [17] J. M. Marshall and C. E. Taylor, "Malaria control with transgenic mosquitoes," *PLoS Med*, vol. 6, no. 2, p. e1000020, 2009.
- [18] C. A. Hill, F. C. Kafatos, S. K. Stansfield, and F. H. Collins, "Arthropod-borne diseases: vector control in the genomics era," *Nature Reviews Microbiology*, vol. 3, no. 3, pp. 262–268, 2005.
- [19] M. O. Ndiath, S. Sougoufara, A. Gaye, C. Mazenot, L. Konate, O. Faye, C. Sokhna, and J.-F. Trape, "Resistance to ddt and pyrethroids and increased kdr mutation frequency in an. gambiae after the implementation of permethrin-treated nets in senegal," *PLoS One*, vol. 7, no. 2, p. e31943, 2012.
- [20] P. Anupa Elizabeth, M. Saravana Mohan, P. Philip Samuel, S. Pandian, and B. Tyagi, "Identification and eradication of mosquito breeding sites using wireless networking and electromechanical technologies," in *Recent Trends in Information Technology (ICRTIT), 2014 International Conference on*. IEEE, 2014, pp. 1–6.
- [21] B. Hur and W. Eisenstadt, "Low-power wireless climate monitoring system with rfid security access feature for mosquito and pathogen research," in *Mobile and Secure Services (MOBISECSERV), 2015 First Conference on*. IEEE, 2015, pp. 1–5.
- [22] J.-T. Ameyo, D. Phelps, O. Oladipo, F. Sewovoe-Ekuoe, S. Jadoonanan, S. Jadoonanan, T. Tabassum, S. Gnabode, T. D. Sherpa, M. Falzone *et al.*, "Medizdroids project: Ultra-low cost, low-altitude, affordable and sustainable uav multicopter drones for mosquito vector control in malaria disease management," in *Global Humanitarian Technology Conference (GHTC), 2014 IEEE*. IEEE, 2014, pp. 590–596.
- [23] C. Boonsri, S. Sumriddetchkajorn, and P. Buranasiri, "Laser-based mosquito repelling module," in *Photonics Global Conference (PGC), 2012*. IEEE, 2012, pp. 1–4.
- [24] J. Kare and J. Buffum, "Build your own photonic fence to zap mosquitoes midflight [backwards star wars]," *IEEE Spectrum*, vol. 5, no. 47, pp. 28–33, 2010. [Online]. Available: <http://spectrum.ieee.org/consumer-electronics/gadgets/backyard-star-wars>
- [25] M. Burbage, S. Manzoor, and A. T. Becker. (2016, Sep.) Mosquito Drone Coverage and Elimination, MATLAB Central File Exchange. [Online]. Available: <http://www.mathworks.com/matlabcentral/fileexchange/59142>
- [26] A. T. Becker, "Unmanned mosquito elimination vehicles," US Patent 62/324,625, 04 19, 2016.
- [27] R. Sollenberger, "Solo specs: Just the facts," May 2015. [Online]. Available: <https://3dr.com/solo-gopro-drone-specs/>

- [28] M. Gillies and T. Wilkes, “The vertical distribution of some West African mosquitoes (Diptera, Culicidae) over open farmland in a freshwater area of The Gambia,” *Bulletin of entomological research*, vol. 66, no. 01, pp. 5–15, 1976.
- [29] A. Schneider, “Gps visualizer,” Mar. 2003. [Online]. Available: <http://www.gpsvisualizer.com>